






Transdisciplinary Visualization of Aortic Dissections

G. Mistelbauer¹, K. Bäumlner¹, D. Mastrodicasa¹, L. D. Hahn², A. Pepe³, V. Sandfort¹, V. Hinostrza¹, K. Ostendorf⁴, A. Schroeder⁴, A. M. Sailer¹, M. J. Willemink¹, S. Walters⁵, B. Preim⁴, and D. Fleischmann¹

¹Department of Radiology, Stanford University School of Medicine, Stanford, CA, USA

²Department of Radiology, University of California San Diego School of Medicine, CA, USA

³Graz University of Technology, Institute of Computer Graphics and Vision, Graz, Austria

⁴Department of Simulation and Graphics, Otto-von-Guericke University Magdeburg, Germany

⁵3D and Quantitative Imaging Laboratory, Stanford, CA, USA

Abstract

Aortic dissection is a life-threatening condition caused by the abrupt formation of a secondary blood flow channel within the vessel wall. Patients surviving the acute phase remain at high risk for late complications, such as aneurysm formation and aortic rupture. The timing of these complications is variable, making long-term imaging surveillance crucial for aortic growth monitoring. Morphological characteristics of the aorta, its hemodynamics, and, ultimately, risk models impact treatment strategies. Providing such a wealth of information demands expertise across a broad spectrum to understand the complex interplay of these influencing factors. We present results of our longstanding transdisciplinary efforts to confront this challenge. Our team has identified four key disciplines, each requiring specific expertise overseen by radiology: lumen segmentation and landmark detection, risk predictors and inter-observer analysis, computational fluid dynamics simulations, and visualization and modeling. In each of these disciplines, visualization supports analysis and serves as communication medium between stakeholders, including patients. For each discipline, we summarize the work performed, the related work, and the results.

CCS Concepts

• **Applied computing** → Life and medical sciences; • **Human-centered computing** → Visualization; • **Computing methodologies** → Computer graphics; Modeling and simulation; Machine learning;

1. Introduction

Visualization of vascular structures is a well-established field with a large body of research, literature, and applications. Aortic dissection poses unique challenges based on the formation of a secondary blood flow channel in the aortic media layer and governed by a thin elastic membrane (dissection flap) that separates the two flow channels (true and false lumen). They are also characterized by diverse cross-sectional shape configurations and longitudinal luminal formations.

A comprehensive perspective and understanding of the pathophysiology of aortic dissection requires a wealth of data that is analyzed and visualized in a meaningful way. Imaging biomarkers from computed tomography angiography (CTA) data, aortic zones, landmarks, the dissection extent, and intermediate luminal communications (connections between true and false lumen) need to be identified and quantified. Phase-contrast magnetic resonance imaging (4D Flow) data and computational fluid dynamics (CFD) simulations can be used to simulate and evaluate blood flow to study its impact on disease progression. Since aortic dissections require lifelong monitoring, these data help to stratify treatment strategies for patients with chronic dissection. In particular, to predict late adverse events and mitigate long-term risk by preventive thoracic endovascular aortic repair (TEVAR). Providing patients with a visual representation

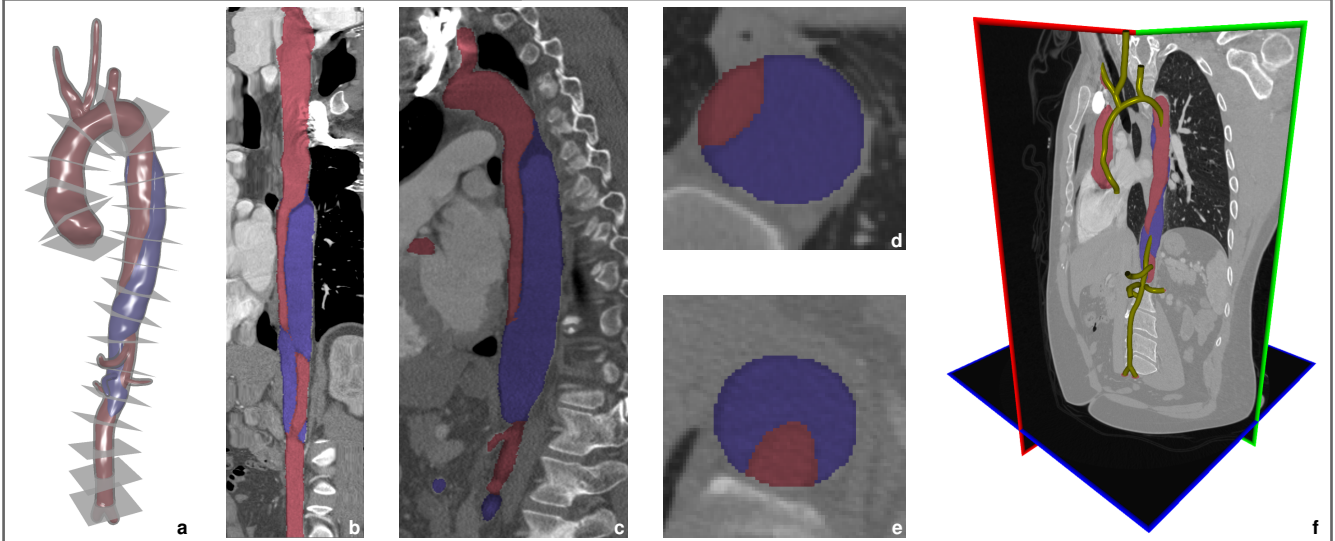
of their current aortic status and its implications for the future could increase their confidence in the treatment process. A comprehensive overview of such approaches is given by Pepe et al. [PLRP*20].

The implementation of such a research venture requires a team of dedicated experts from different disciplines. Such disciplines include, among others, computer vision, machine learning, data science, biomechanics, hemodynamics, and computer graphics, all coordinated according to radiology requirements. Our transdisciplinary journey towards a comprehensive understanding of aortic dissection starts with segmentation or labeling of data, followed by analysis and simulation, and finally visualization of intermediate or aggregate results (see Figure 1). Often, this is not a straightforward process, but an iterative one. The following sections detail our endeavor and describe challenges we addressed.

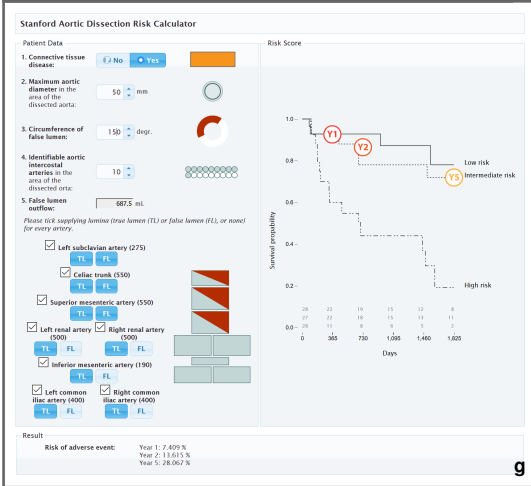
2. Segmentation, Landmark Detection, and Virtual Dissections

Extracting information from imaging data is an essential step (see Figure 1a-f). Visualizations are often based on the segmented data, CFD simulations directly build upon segmentations, and risk prediction models could be streamlined with automated segmentation and feature extraction. For that reason, we reviewed machine learning approaches to segment aortic dissections [MCB*22].

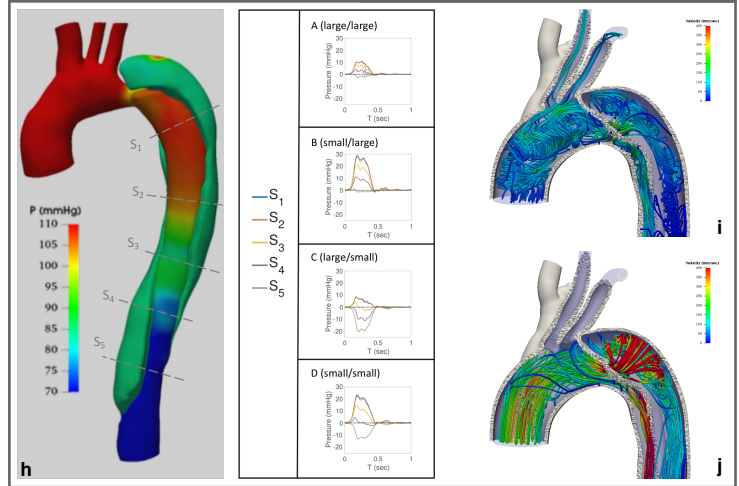
Segmentation, Landmark Detection, and Virtual Dissections



Risk Predictors and Inter-observer Reproducibility Analysis



Computational Fluid Dynamics Simulations



Visualization and Modeling

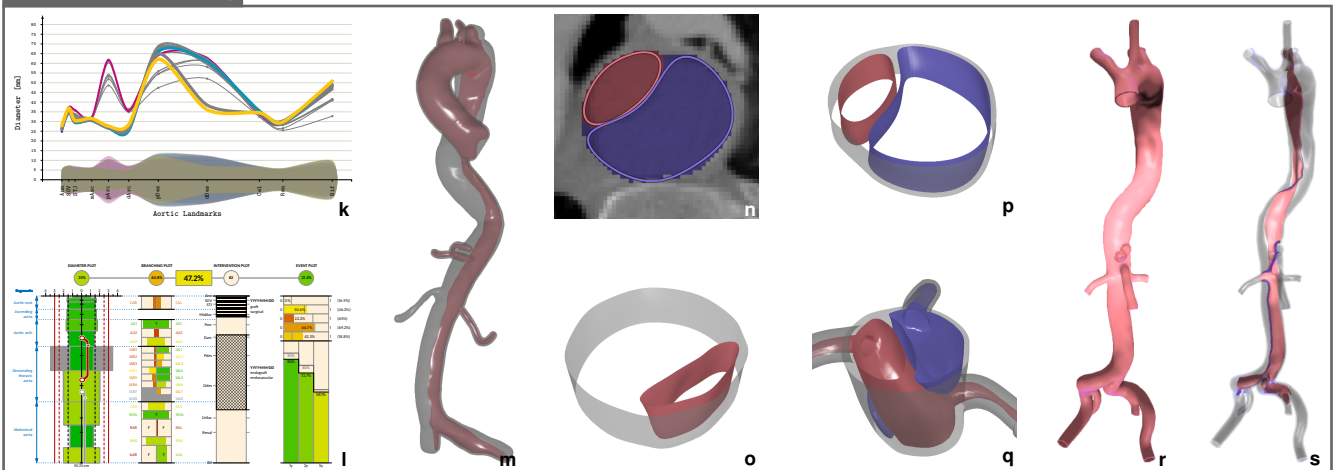


Figure 1: Overview of our transdisciplinary work on visualization for aortic dissection. (l) is taken from [MSS* 16] and © The Author(s) Eurographics Proceedings © 2016 The Eurographics Association.

To segment true and false lumen, we started with a deep-learning approach that locates the entire aorta and extracts its centerline [HMH*20]. Subsequently, the aortic volume was resampled along its centerline (gray cross-sections in Figure 1a) and both flow channels were segmented using a convolutional neural network (CNN), as displayed in Figure 1b-e with the true lumen in red and false lumen in blue. The study comprised 153 CTA data sets from 45 patients with uncomplicated type-B aortic dissection. We then compared different CNN models for segmenting both lumen and false lumen thrombosis, on 40/147 and 27/93 patients/scans, respectively [WCM*21].

The aorta can be divided into 5 segments and 8–11 landmarks [TSCA*20]. The aortic annulus is the first landmark, and its position plays an important role in aortic valve repair, diameter measurement, or aortic centerlines. We trained a deep reinforcement agent to automatically localize the annulus in patients with dissections [CPM*20]. The study comprised 99 scans from 90 patients.

To better understand the formation of a dissection, it would be optimal to know the condition of the aorta prior to dissection. Since patients usually present after experiencing acute symptoms, most already suffer from dissection. For this reason, the collection of data prior to dissection is largely incidental. We made a first attempt to overcome this problem by regressing a virtual pre-dissection data set [PMG*20]. Training was performed on 75 healthy scans and tested on 52 dissection cases.

Related Work. The segmentation of vascular structures is an established field with a plethora of algorithms. Feiger et al. [FLSC*21] reviewed approaches to segment aortic dissections based on U-Nets. A multi-stage learning approach that also segments aortic branches was described by Chen et al. [CZM*21]. Hata et al. [HYY*21] segmented aortic dissections in non-contrast-enhanced computed tomography (CT) data.

Outcome. Our work addresses several image segmentation challenges specific to aortic dissections. Among these, the segmentation of the true and false lumen with a first attempt to segment false lumen thrombosis. This reduces the need for manual segmentation and paves the way towards aortic modeling and cross-sectional shape analysis. Combined with the virtual pre-dissection and the aortic annulus localization, we are one step closer to a comprehensive, automatic extraction of aortic dissections from imaging data.

3. Risk Predictors and Inter-observer Reproducibility Analysis

At the core of numerous clinical research on aortic dissection is the prediction of late adverse events and patient-specific outcomes. These models are often based on morphological features that are derived from medical images and, thus, rely on accurate and reproducible methods for their extraction. In a retrospective study including 83 patients with uncomplicated type-B aortic dissection, we correlated several imaging and morphological characteristics with late adverse events [SvKN*17]. These characteristics are based on CTA data and the following four were found to be significant predictors of late adverse events: maximum aortic diameter, false lumen circumferential angle, false lumen outflow, and number of intercostal arteries along the dissected aorta.

The measurement variability of these four imaging predictors was later evaluated in a retrospective study of 72 patients with uncomplicated type-B aortic dissection by four independent observers [WMM*23]. Three experiments were conducted. Firstly, observers were asked to use the same postprocessing software without a workflow. Secondly, observers were instructed to follow a standardized imaging workflow. In the third experiment, observers had a training session with consensus reading on how to perform measurements before using the standardized workflow. Results were compared to estimate the effect of a standardized workflow and a training session on the reproducibility of aortic measurements.

One of our research projects mimicked the way radiology technologists estimate double-oblique measurement planes at landmark locations along the aorta [PEC*21]. Combining a CNN-based approach with uncertainty quantification, these cross-sections can be learned from imperfect data and estimated with higher reproducibility. Diameter data were collected in 162 CT scans from 147 patients by one out of 11 radiology technologists at 11 aortic landmarks. To assess the inter-observer variability, 12 scans were processed by three technologists.

Related Work. In general, the reproducibility of aortic measurements is critically viewed because of inter- and intra-observer variability [NCS*16]. Elliptic Fourier descriptor (EFD) of the true lumen were used to assess enlargement of type-B aortic dissections [SIK*17].

Outcome. A risk model to predict late adverse events in patients with uncomplicated type-B aortic dissection was developed (see Figure 1g). The numerous characteristics that were investigated in this study constitute the foundation for the aortic dissection map visualization [MSS*16]. Standardized procedures can reduce the inter-observer variability of aortic measurements. Additional training time on such protocols leads to even better results.

4. Computational Fluid Dynamics Simulations

In addition to morphological characteristics, hemodynamic features are related to late adverse events, individual patient outcomes, and may ultimately inform treatment decisions. However, obtaining patient-specific hemodynamic information is challenging, with 4D Flow and CFD being the two main approaches used to date.

We performed fluid-structure interaction (FSI) simulations on patient-specific geometries based on CTA data and informed the boundary conditions with functional data of the same patient extracted from *in vivo* 4D Flow [BVS*20], as shown in Figure 1i-j. Taking the structural domain into account allowed us to account for the mechanics and deformation of the vessel wall and dissection flap during the cardiac cycle, which in turn affect flow and pressure in the fluid domain. We further investigated the effect of intimal flap stiffness on flap displacement, pressure differences between true and false lumen, and wall shear stress.

Numerical simulations lend themselves naturally to *in silico* scenarios and allowed us investigate the effect of morphological changes (entry and exit tear size) and flap mobility on false lumen pressurization and flow rates [BZE*23], as shown in Figure 1h. A

rigid vessel wall increased true lumen flow rates and pressure differences between true and false lumen, highlighting the importance of accurately capturing tissue elasticity. The simulations confirmed that increased resistance to false lumen drainage, caused by a reduction in exit tear size, increased the pressure in the false lumen.

Related Work. Markevi et al. [MSK*21] correlated *in vivo* 4D Flow derived metrics with aortic growth in a cohort of 12 patients with type-B aortic dissection. The authors found that increased false lumen ejection fraction and a reduced pressure drop between proximal and distal aorta were related to aortic growth. In another study, Xu et al. [XXH*21] performed CFD simulations on 51 patients at initial presentation and after TEVAR. The authors developed a hemodynamic index based on the location of pressure equilibrium between true and false lumen, and found a correlation with functional improvement after TEVAR.

Outcome. Hemodynamic factors contribute to the progression of aortic dissection. Even though hemodynamic data are not routinely generated in clinical care, CFD and FSI simulations are increasingly employed to obtain and examine patient-specific hemodynamic features non-invasively. Several studies with *in silico* scenarios or in patient cohorts were able to elucidate the complex interplay of morphological and hemodynamic features and their relation to patient outcome, indicating the potential value of a hemodynamic assessment of patients with aortic dissections. A sophisticated and clear visualization of key hemodynamic factors will convey important findings to medical experts and facilitate translational research.

5. Visualization and Modeling

The amount of extracted, generated, and simulated information requires tailored visualization, especially if the intention is to make these data accessible to clinical and patient care. As a first clinically implemented program, we designed the *aortic surveillance program*, a concise and standardized 2D diagram of the aortic diameter progression [MSS*17], shown in Figure 1k. Aiming at effective communication with patients, time is encoded in the pen's width and color highlights important dates, such as before and after an intervention or the current aortic state. So far, this diagram is used about 10 times per day in the clinical routine. Equipped with additional dissection information, we introduced aortic dissection maps (see Figure 1l), a combination of four distinctive, vertically-arranged plots, the diameter, branching, intervention, and event plot [MSS*16]. Diameters can be compared with one preceding intervention and false lumina are depicted as branching lines from the true lumen. Branching information shows the connectivity of a branch to its parent lumen including the amount of blood inflow and outflow. The number and type of interventions are depicted in the third plot and the risk of late adverse events is shown last. All these different data provide a concise yet essential snapshot of a patient's aortic state. The event plot is based on our risk model [SvKN*17], which again highlights the transdisciplinary nature of our work. We then focused on the temporal development of the aortic dissection landmarks-diameter (x and y -axis) plot by warping space to view time [SFP*19]. Using an ellipsoidal coordinate system instead of a Cartesian one, we can make the time successively apparent when viewing the diagram from the side, i.e., the time (z -axis) emerges from the image plane.

The topology of aortic dissections is often complex and difficult to assess on medical imaging. Based on segmentations, our goal was to create a clear representation of the outer vessel wall and the dissection flap, which poses specific visualization challenges. We used EFDs to capture the true and false lumen cross-sectional shape variability and combined them with implicit modelling to reconstruct the surface of the aorta and its branches [MRB*21], as shown in Figure 1m-q. This leads to one surface for the true and false lumen inner wall, including communications between them, and another surface for the outer vessel wall. Visualizing such geometries of inner and outer aortic surfaces with the dissection flap was subsequently investigated [OMB*21], as shown in Figure 1r-s. By combining different diffuse (Blinn-Phong, Oren-Nayar, toon) and specular (Blinn-Phong, Cook-Torrance, toon) shading styles with ambient occlusion and the Fresnel effect, modulated with transparency, we created a visualization gallery of aortic dissections.

Related Work. Analogously to segmentation of vascular structures, their visualization is also an extensive field. It ranges from 2D visualizations (e.g., projections [MMV*13]) to 3D visualization approaches categorized into model-based and model-free, both being either explicit and implicit [MRB*21].

Outcome. Through visualization, we addressed the challenge of displaying multivariate data over time while maintaining the spatial orientation of the aorta as much as possible. This was accomplished in 2D either with concise and standardized maps, or in 2.5D to visualize time through interaction. We modeled and reconstructed the aortic dissection including its inner and outer vessel walls in 3D, while preserving the luminal separation through the dissection flap. The preferred rendering style for the complex dissection anatomy was a semi-transparent wall with Fresnel effect and a flap with Oren-Nayar and Cook-Torrance. This allows inspection of the dissection flap, while the aortic wall serves as context.

6. Conclusion and Future Work

Aortic dissection is a complex disease that exhibits a high degree of variability. To make an in-depth and holistic assessment, pursuing transdisciplinary research is paramount. We studied the following principal aspects: segmentation using CNNs, risk model development, inter-observer variability analysis, measurement plane estimation, CFD simulations, visualization of diameters and multiple aortic characteristics, modeling of true and false lumen cross-sectional shapes, and their rendering using different styles. In this diverse work, visualization can act as a unifying discipline to communicate findings within the research team, to professionals, and to patients.

Although considerable work was done, each of these individual steps can be improved. We could directly segment true and false lumen and possibly their surface. The predictive value of the true and false lumen shapes could be investigated. Flow visualizations of CFD simulations, including the true and false lumen geometry, are another promising future avenue.

References

- [BVS*20] BÄUMLER K., VEDULA V., SAILER A. M., SEO J., CHIU P., MISTELBAUER G., CHAN F. P., FISCHBEIN M. P., MARSDEN A. L.,

- FLEISCHMANN D.: Fluid-structure interaction simulations of patient-specific aortic dissection. *Biomech Model Mechanobiol* 19, 5 (2020), 1607–1628. doi:10.1007/s10237-020-01294-8. 3
- [BZE*23] BÄUMLER K., ZIMMERMANN J., ENNIS D. B., MARSDEN A. L., FLEISCHMANN D.: Hemodynamic Effects of Entry Versus Exit Tear Size and Tissue Stiffness in Simulations of Aortic Dissection. In *Computer Methods, Imaging and Visualization in Biomechanics and Biomedical Engineering II*, vol. 38. 2023, pp. 143–152. doi:10.1007/978-3-031-10015-4. 3
- [CPM*20] CODARI M., PEPE A., MISTELBAUER G., MASTRODICASA D., WALTERS S., WILLEMINK M. J., FLEISCHMANN D.: Deep reinforcement learning for localization of the aortic annulus in patients with aortic dissection. In *Proc. of the Workshop on Thoracic Image Analysis* (2020), vol. 12502, pp. 94–105. doi:10.1007/978-3-030-62469-9_9. 3
- [CZM*21] CHEN D., ZHANG X., MEI Y., LIAO F., AN ZHENFENG LI H. X., XIAO Q., GUO W., ZHANG H., YAN T., XIONG J., VENTIKOS Y.: Multi-stage learning for segmentation of aortic dissections using a prior aortic anatomy simplification. *Med Image Anal* 69 (2021), 101931:1–101931:12. doi:10.1016/j.media.2020.101931. 3
- [FLSC*21] FEIGER B., LORENZANA-SALDIVAR E., COOKE C., HORSTMAYER R., BISHAWI M., DOBERNE J., HUGHES G. C., RANNEY D., VOIGT S., RANGLES A.: Evaluation of U-Net based architectures for automatic aortic dissection segmentation. *ACM Trans Comput Healthc* 3, 1 (2021), 11:1–11:16. doi:10.1145/3472302. 3
- [HMH*20] HAHN L. D., MISTELBAUER G., HIGASHIGAITO K., KOCI M., WILLEMINK M. J., SAILER A. M., FISCHBEIN M., FLEISCHMANN D.: CT-based true- and false-lumen segmentation in type B aortic dissections using machine learning. *Radiology: Cardiothoracic Imaging* 2, 3 (2020), e190179. doi:10.1148/ryct.2020190179. 3
- [HYY*21] HATA A., YANAGAWA M., YAMAGATA K., SUZUKI Y., KIDO S., AMD SHUHEI DOI A. K., YOSHIDA Y., MIYATA T., TSUBAMOTO M., KIKUCHI N., TOMIYAMA N.: Deep learning algorithm for detection of aortic dissection on non-contrast-enhanced CT. *Eur Radiol* 31, 2 (2021), 1151–1159. doi:10.1007/s00330-020-07213-w. 3
- [MCB*22] MASTRODICASA D., CODARI M., BÄUMLER K., SANDFORT V., SHEN J., MISTELBAUER G., HAHN L. D., TURNER V. L., DESJARDINS B., WILLEMINK M. J., FLEISCHMANN D.: Artificial intelligence applications in aortic dissection imaging. *Semin Roentgenol* 57, 4 (2022), 357–363. doi:10.1053/j.ro.2022.07.001. 1
- [MMV*13] MISTELBAUER G., MORAR A., VARCHOLA A., SCHERNTHANER R., BAČLIJA I., KÖCHL A., KANITSAR A., BRUCKNER S., GRÖLLER M. E.: Vessel visualization using curvilinear feature aggregation. *Computer Graphics Forum* 32, 3 (2013), 231–240. doi:10.1111/cgf.12110. 4
- [MRB*21] MISTELBAUER G., RÖSSL C., BÄUMLER K., PREIM B., FLEISCHMANN D.: Implicit modeling of patient-specific aortic dissections with elliptic fourier descriptors. *Computer Graphics Forum* 40, 3 (2021), 423–434. doi:10.1111/cgf.14318. 4
- [MSK*21] MARLEVI D., SOTELO J. A., KAYLOR R. G., AHMED Y., URIBE S., PATEL H. J., EDELMAN E. R., NORDSLETEN D. A., BURRIS N. S.: False lumen pressure estimation in type B aortic dissection using 4D flow cardiovascular magnetic resonance: comparisons with aortic growth. *Journal of Cardiovascular Magnetic Resonance* (2021), 1–13. doi:10.1186/s12968-021-00741-4. 4
- [MSS*16] MISTELBAUER G., SCHMIDT J., SAILER A.-M., BÄUMLER K., WALTERS S., FLEISCHMANN D.: Aortic dissection maps: Comprehensive visualization of aortic dissections for risk assessment. In *Proc. of Eurographics Workshop on Visual Computing for Biology and Medicine* (2016), pp. 143–152. doi:10.2312/vcbm.20161282. 2, 3, 4
- [MSS*17] MISTELBAUER G., SCHMIDT J., SAILER A.-M., WALTERS S., FLEISCHMANN D.: Visualization of aortic diameter changes over time in an aortic surveillance program. In *Proc. of the ECR Book of Abstracts* (2017), pp. C–1905. doi:10.1594/ecr2017/C-1905. 4
- [NCS*16] NIENABER C. A., CLOUGH R. E., SAKALIHASAN N., SUZUKI T., GIBBS R., MUSSA F., JENKINS M. P., THOMPSON M. M., EVANGELISTA A., YEH J. S. M., CHESHIRE N., ROSENDAHL U., PEPPER J.: Aortic dissection. *Nature Reviews Disease Primers* 2 (2016), 16053:1–16053:18. doi:10.1038/nrdp.2016.53. 3
- [OMB*21] OSTENDORF K., MASTRODICASA D., BÄUMLER K., CODARI M., TURNER V., WILLEMINK M. J., FLEISCHMANN D., PREIM B., MISTELBAUER G.: Shading style assessment for vessel wall and lumen visualization. In *Proc. of Eurographics Workshop on Visual Computing for Biology and Medicine (Short Papers)* (2021), pp. 107–111. doi:10.2312/vcbm.20211350. 4
- [PEC*21] PEPE A., EGGER J., CODARI M., WILLEMINK M. J., GSAXNER C., LI J., ROTH P. M., MISTELBAUER G., SCHMALSTIEG D., FLEISCHMANN D.: Automated cross-sectional view selection in CT angiography of aortic dissections with uncertainty awareness and retrospective clinical annotations, 2021. doi:10.48550/ARXIV.2111.11269. 3
- [PLRP*20] PEPE A., LI J., ROLF-PISSARCZYK M., GSAXNER C., CHEN X., HOLZAPFEL G. A., EGGER J.: Detection, segmentation, simulation and visualization of aortic dissections: A review. *Med Image Anal* 65 (2020), 101931:1–101931:16. doi:10.1016/j.media.2020.101931. 1
- [PMG*20] PEPE A., MISTELBAUER G., GSAXNER C., LI J., FLEISCHMANN D., SCHMALSTIEG D., EGGER J.: Semi-supervised virtual regression of aortic dissections using 3D generative inpainting. In *Proc. of the Workshop on Thoracic Image Analysis* (2020), vol. 12502, pp. 130–140. doi:10.1007/978-3-030-62469-9_12. 3
- [SFP*19] SCHMIDT J., FLEISCHMANN D., PREIM B., BRÄNDLE N., MISTELBAUER G.: Popup-plots: Warping temporal data visualization. *IEEE Trans Vis Comput Graph* 25, 7 (2019), 2443–2457. doi:10.1109/TVCG.2018.2841385. 4
- [SIK*17] SATO H., ITO T., KURODA Y., UCHIYAMA H., WATANABE T., YASUDA N., NAKAZAWA J., HARADA R., KAWAHARADA N.: New predictor of aortic enlargement in uncomplicated type B aortic dissection based on elliptic Fourier analysis. *Eur J Cardiothorac Surg* 52, 6 (2017), 1118–1124. doi:10.1093/ejcts/ezx191. 3
- [SvKN*17] SAILER A. M., VAN KUIJK S. M. J., NELEMANS P., CHIN A. S., KINO A., HUININGA M., SCHMIDT J., MISTELBAUER G., BÄUMLER K., CHIU P., FISCHBEIN M. P., DAKE M. D., MILLER D. C., SCHURINK G. W. H., FLEISCHMANN D.: Computed tomography imaging features in acute uncomplicated Stanford type-B aortic dissection predict late adverse events. *Circulation Cardiovascular Imaging* 10:e005709, 4 (2017). doi:10.1161/CIRCIMAGING.116.005709. 3, 4
- [TSCA*20] TAHOCES P. G., SANTANA-CEDRÉS D., ALVAREZ L., ALEMÁN-FLORES M., TRUJILLO A., CUENCA C., CARREIRA J. M.: Automatic detection of anatomical landmarks of the aorta in CTA images. *Medical & Biological Engineering & Computing* 58 (2020), 903–919. doi:10.1007/s11517-019-02110-x. 3
- [WCM*21] WOBLEN L. D., CODARI M., MISTELBAUER G., PEPE A., HIGASHIGAITO K., HAHN L. D., MASTRODICASA D., TURNER V. L., HINOSTROZA V., BÄUMLER K., FISCHBEIN M. P., FLEISCHMANN D., WILLEMINK M. J.: Deep learning-based 3D segmentation of true lumen, false lumen, and false lumen thrombosis in type-B aortic dissection. In *Proc. IEEE Engineering in Medicine & Biology Society* (2021), pp. 3912–3915. doi:10.1109/EMBC46164.2021.9631067. 3
- [WMM*23] WILLEMINK M. J., MASTRODICASA D., MADANI M. H., CODARI M., CHEPELEV L. L., MISTELBAUER G., HANNEMAN K., OUZOUNIAN M., OCAZONEZ D., AFIFI R. O., LACOMIS J. M., LOVATO L., PACINI D., FOLESANI G., HINZPETER R., ALKADHI H., STILLMAN A. E., SAILER A. M., TURNER V. L., HINOSTROZA V., BÄUMLER K., CHIN A. S., BURRIS N. S., MILLER D. C., FISCHBEIN M. P., FLEISCHMANN D.: Inter-observer variability of expert-derived morphologic risk predictors in aortic dissection. *Eur Radiol* 33, 2 (2023), 1102–1111. doi:10.1007/s00330-022-09056-z. 3
- [XXH*21] XU H., XIONG J., HAN X., MEI Y., SHI Y., WANG D., ZHANG M., CHEN D.: Computed tomography-based hemodynamic index for aortic dissection. *J Thorac Cardiovasc Surg* 162, 2 (2021), e165–e176. doi:10.1016/j.jtcvs.2020.02.034. 4